The Astrophysical Journal, 761:134 (6pp), 2012 December 20 doi:10.1088/0004-637X/761/2/134

SAUSAGE OSCILLATIONS OF CORONAL PLASMA STRUCTURES

V. M. Nakariakov[1,2], C. Hornsey[1], and V. F. Melnikov[2]
[1] Physics Department, University of Warwick, Coventry CV4 7AL, UK
[2] Central Astronomical Observatory at Pulkovo of the Russian Academy of Sciences, 196140 St Petersburg, Russia; V.Nakariakov@warwick.ac.uk
Received 2012 August 17; accepted 2012 October 30; published 2012 December 4

ABSTRACT

The dependence of the period of sausage oscillations of coronal loops on length together with the depth and steepness of the radial profile are determined. We performed a parametric study of linear axisymmetric fast magnetoacoustic (sausage) oscillations of coronal loops modeled as a field-aligned low-β plasma cylinder with a smooth inhomogeneity of the plasma density in the radial direction. The density decreases smoothly in the radial direction. Sausage oscillations are impulsively excited by a perturbation of the radial velocity, localized at the cylinder axis and with a harmonic dependence on the longitudinal coordinate. The initial perturbation results in either a leaky or a trapped sausage oscillation, depending upon whether the longitudinal wavenumber is smaller or greater than a cutoff value, respectively. The period of the sausage oscillations was found to always increase with increasing longitudinal wavelength, with the dependence saturating in the long-wavelength limit. Deeper and steeper radial profiles of the Alfvén speed correspond to more efficient trapping of sausage modes: the cutoff value of the wavelength increases with the steepness and the density (or Alfvén speed) contrast ratio. In the leaky regime, the period is always longer than the period of a trapped mode of a shorter wavelength in the same cylinder. For shallow density profiles and shorter wavelengths, the period increases with wavelength. In the long-wavelength limit, the period becomes independent of the wavelength and increases with the depth and steepness of the radial profile of the Alfvén speed.

Key words: Sun: flares – Sun: oscillations – Sun: radio radiation – Sun: X-rays, gamma rays

1. INTRODUCTION

The theoretical foundation of magnetohydrodynamic (MHD) coronal seismology, the rapidly developing branch of solar physics that uses MHD waves and oscillations for plasma diagnostics, is the theory of MHD oscillations of a plasma cylinder (see, e.g., Banerjee et al. 2007; De Moortel & Nakariakov 2012; Stepanov et al. 2012, for recent reviews). This model adequately describes standing and propagating MHD waves in various plasma structures of the solar corona, such as loops and various filaments. In the low-β plasma, typical of coronal active regions, a plasma cylinder embedded in a plasma with different properties has four main modes: torsional, kink, sausage, and longitudinal modes (e.g., Zaitsev & Stepanov 1975, 1982; Edwin & Roberts 1983). These modes have very different physical properties and different observational manifestations. The sausage mode, also known as an $m = 0$ or peristaltic mode, is a sequence of expansions and contractions of the cross-section of the cylinder, accompanied by a variation in the plasma density and in the absolute value of the magnetic field. In a low-β case the plasma flows in the sausage mode are predominantly transverse, in the radial direction (e.g., Gruszecki et al. 2012).

Initial interest in the sausage mode was associated with the medium-period quasi-periodic pulsations observed in flaring energy releases (e.g., Rosenberg 1970; Zaitsev & Stepanov 1982; Nakariakov & Melnikov 2009). The first direct spatially resolved observational detection of a sausage oscillation of a flaring loop was made in the gyrosynchrotron and soft X-ray emission (Nakariakov et al. 2003; Melnikov et al. 2005). Detailed analysis of the possible examples of sausage oscillations showed good spatial coherence of the oscillatory signals over the whole loop spatially resolved in the microwave band (Inglis et al. 2008). Such a spatial structure is consistent with the sausage mode, while alternative interpretations, e.g., in terms of the "dripping" model (Nakariakov & Melnikov 2009), cannot be excluded. Analysis of the optical emission from a cool post-flare loop revealed the possible presence of the global (fundamental) sausage mode as well as its second spatial harmonic (Srivastava et al. 2008). Sausage oscillations could also be responsible for the intensity oscillations observed in the gradual phase of a white-light flare on the RS CVn binary II Peg (Mathioudakis et al. 2003). Very recently, periodic variations of the EUV emission were also interpreted in terms of sausage oscillations (Van Doorsselaere et al. 2011; Su et al. 2012). In these interpretations it is important to pay attention to the line-of-sight integration effect, as recently pointed out by Mossessian & Fleishman (2012) and Gruszecki et al. (2012). In particular, for a line of sight perpendicular to the oscillating cylinder and for a spatial resolution of the order of the diameter of the cylinder or poorer, the intensity perturbations produced by a sausage mode in the optically thin emission regime are negligible. Theoretical modeling of sausage modes of coronal structures has a long history. Sausage modes are highly dispersive and their properties are dependent upon the longitudinal wavenumber (e.g., Zaitsev & Stepanov 1982; Edwin & Roberts 1983; Roberts et al. 1984; Selwa et al. 2004). Depending upon the ratio of the longitudinal wavelength (determined, e.g., in the case of standing waves by the length of the oscillating loop) to the radius of the plasma cylinder, the mode can be either trapped or leaky. Trapped modes experience total internal reflection at the cylinder surface and are evanescent outside the loop. The period of standing trapped sausage modes, i.e., in dense and thick flaring loops, grows with wavelength (Nakariakov et al. 2003; Aschwanden et al. 2004). Sausage modes of longer wavelengths leak from the cylinder, forming a train of outwardly propagating fast magnetoacoustic waves outside the cylinder. This mechanism of wave leakage is intrinsic and different from the tunneling caused by non-uniformity of the external medium (see, e.g., Verwichte et al. 2006). The threshold value of the ratio of the longitudinal wavelength to the radius of the cylinder is defined by the ratio of the fast magnetoacoustic speeds inside and outside the cylinder (Zaitsev & Stepanov 1982; Edwin & Roberts 1983). Such a behavior was

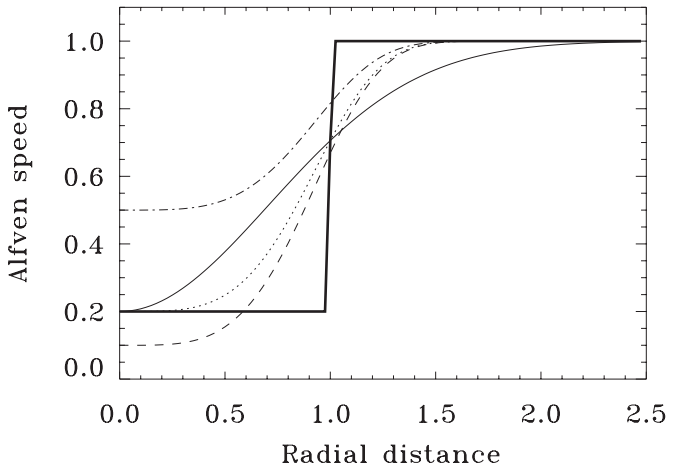

Figure 1. Examples of the radial profiles of the Alfvén speed in the plasma cylinder considered for different values of the parameters α and δ, which control the steepness and depth of the profile, respectively. The thick solid curve corresponds to $\alpha = \infty$, $\delta = 0.8$, the thin solid curve to $\alpha = 2$, $\delta = 0.8$, the dotted curve to $\alpha = 4$, $\delta = 0.8$, the dashed curve to $\alpha = 4$, $\delta = 0.9$, and the dot-dashed curve to $\alpha = 4$, $\delta = 0.5$. The Alfvén speed is normalized to its value at infinity and the radial distance is normalized to the effective radius of the cylinder.

found to be weakly sensitive to the smoothness of the transverse profile of the fast speed (Pascoe et al. 2007b), fine structure in the form of multiple coaxial shells (Pascoe et al. 2007a), longitudinal variation of the cylinder cross-section (Pascoe et al. 2009), and finite-β effects (Inglis et al. 2009).

However, sausage modes are still not entirely understood. In particular, the dependence of the time period on the longitudinal wavelength in the leaky regime, information crucial for the development of seismological techniques based upon this mode, is still debated. On the one hand, analysis of dispersion relations for linear sausage perturbations clearly showed that in the long-wavelength regime the period of leaky sausage modes is independent of wavelength (e.g., Zaitsev & Stepanov 1982; Cally 1986; Kopylova et al. 2002, 2007) and is determined by the ratio of the radius of the cylinder to the internal value of the fast speed. On the other hand, it was argued that the gradual increase in wavelength from a trapped regime value should lead to an increase in the period (Nakariakov et al. 2003; Aschwanden et al. 2004) for a fixed value of the radius of the cylinder. Moreover, numerical simulations of the initial-value problem demonstrated that the period of the mode grows with wavelength (e.g., Pascoe et al. 2007b; Inglis et al. 2009) in both trapped and leaky regimes. The situation is complicated by difficulties in searching analytically for the complex roots of the transcendental algebraic equations representing the dispersion relations (Ruderman & Roberts 2006).

In this paper we aim to resolve this long-standing discrepancy. We analyze an initial-value problem, considering the evolution of an axially symmetric perturbation of a straight plasma cylinder embedded in a uniform magnetic field, as in the works of Pascoe et al. (2007b), Inglis et al. (2009), and Gruszecki et al. (2012). In contrast to Pascoe et al. (2007b) and Inglis et al. (2009), where a plane plasma slab was considered, we study sausage modes of a plasma cylinder. Moreover, we extend the range of the parameters of the problem, considering ratios of the length of the perturbed cylinder to its diameter up to 60 and ratios of the Alfvén speeds outside and inside the cylinder up to 20. In previous studies these parameters were considered up to 15 and 7, respectively (Inglis et al. 2009). In addition, we study the dependence of the sausage mode period on the steepness of the transverse profile of the plasma in the cylinder.

We consider a radially non-uniform plasma cylinder embedded in a uniform and straight magnetic field in the zero-β regime. We perform a parametric study of the sausage mode of this plasma equilibrium, varying the contrast of the Alfvén (fast magnetoacoustic) speed inside and outside the cylinder and the steepness of the plasma non-uniformity in the radial direction. We consider, for the first time, the transition from the short-wavelength trapped regime to the long-wavelength regime, investigating how the dependence of the period on the wavelength evolves to its independence.

2. NUMERICAL MODEL

Consider a smooth cylinder of a zero-β plasma, stretched along a uniform magnetic field B_0 directed in the z-direction. The density of the plasma ρ_0 decreases with the radial coordinate r. This is a standard setup for modeling sausage oscillations of coronal loops: see, e.g., Figures 1 and 2 of Pascoe et al. (2007a). The Alfvén speed (that coincides with the fast speed in this limit) increases in the radial direction and is modeled by the function

$$C_A(r) = B_0/\sqrt{\mu_0\rho_0(r)} = C_{A\infty}\left[1 - \delta\exp\left(-\frac{r^\alpha}{d^\alpha}\right)\right], \quad (1)$$

where $C_{A\infty}$ is the Alfvén speed at infinity, $0 < \delta < 1$ is the decrease in the speed at the axis of the cylinder, $\alpha > 1$ is the index of the steepness of the profile, d is the effective radius of the cylinder (see Figure 1), and μ_0 is the vacuum permeability. The Alfvén speed is then $C_{A0} = C_{A\infty}(1-\delta)$ at the cylinder axis. Thus, by varying the parameters δ and α we change the contrast ratio $C_{A0}/C_{A\infty}$ and the steepness of the radial profile, respectively. As the magnetic field is uniform and the gas pressure is taken to be negligible, the equilibrium total pressure is constant everywhere. Hence, the parameter $\delta = 1 - C_{A0}/C_{A\infty}$ is connected with the contrast of the equilibrium plasma density ρ_0 in the cylinder center and at infinity as $\delta = 1 - [\rho_0(\infty)/\rho_0(0)]^{1/2}$. The case of an infinitely steep profile, $\alpha \to \infty$, corresponds to the Edwin & Roberts (1983) model with a step-function profile.

In this study we restrict our attention to dissipationless processes, described by ideal MHD:

$$\rho\frac{d\mathbf{V}}{dt} = -\frac{1}{\mu_0}\mathbf{B}\times\mathrm{curl}\mathbf{B}, \quad (2)$$

$$\frac{\partial\mathbf{B}}{\partial t} = \mathrm{curl}(\mathbf{V}\times\mathbf{B}), \quad (3)$$

$$\frac{\partial\rho}{\partial t} + \mathrm{div}(\rho\mathbf{V}) = 0, \quad (4)$$

where the vectors $\mathbf{V}$ and $\mathbf{B}$ are the plasma velocity and magnetic field, respectively, and ρ is the plasma density. In Equation (2), we ignore finite-β effects as they are not significant for sausage modes of coronal loops (Inglis et al. 2009).

It is natural to use a cylindrical coordinate system, with the z-axis coinciding with the axis of the cylinder and with ϕ and r the azimuthal and radial coordinates, respectively. Considering linear magnetoacoustic perturbations of the cylindrical equilibrium given by Equation (1); and taking perturbations to be

independent of the polar angle ϕ in the sausage mode, we obtain for the perturbed quantities

$$\frac{\partial v_r}{\partial t} = \frac{B_0}{\mu_0 \rho_0}\left(\frac{\partial B_r}{\partial z} - \frac{\partial B_z}{\partial r}\right), \quad (5)$$

$$\frac{\partial B_r}{\partial t} = B_0 \frac{\partial v_r}{\partial z}, \quad (6)$$

$$\frac{\partial B_z}{\partial t} = -B_0\left(\frac{\partial v_r}{\partial r} + \frac{v_r}{r}\right), \quad (7)$$

where v_r is the radial component of the plasma velocity, and B_r and B_z are the perturbations of the radial and longitudinal components of the magnetic field, respectively.

Using the standard procedure of excluding of all but one perturbed variable from Equations (5)–(7) (see, e.g., the linear part of Nakariakov et al. 1997), we obtain the fast magnetoacoustic wave equation,

$$\frac{\partial^2 v_r}{\partial t^2} = \frac{B_0^2}{\mu_0 \rho_0(r)}\left(\frac{\partial^2 v_r}{\partial z^2} + \frac{\partial^2 v_r}{\partial r^2} + \frac{1}{r}\frac{\partial v_r}{\partial r} - \frac{v_r}{r^2}\right), \quad (8)$$

for sausage perturbations of the field-aligned plasma cylinder. Slow magnetoacoustic perturbations are absent from this equation as we ignore finite-β effects.

As the equilibrium is uniform along the axis of the cylinder (in the z-direction) we can perform the Fourier transform with respect to this coordinate, assuming that the perturbed physical quantities depend upon z as $\cos(k_z z)$. These assumptions correspond to the consideration of standing modes with longitudinal wavelength $2\pi/k_z$. Thus, we obtain the fast wave equation for the harmonic fast magnetoacoustic perturbations in the longitudinal direction,

$$\frac{1}{C_A^2(r)}\frac{\partial^2 v_r}{\partial t^2} + \left(k_z^2 + \frac{1}{r^2}\right)v_r - \frac{\partial^2 v_r}{\partial r^2} - \frac{1}{r}\frac{\partial v_r}{\partial r} = 0. \quad (9)$$

Equation (9) contains explicit dependence upon only two coordinates, the time t and the radial coordinate r. In particular, Equation (9) describes standing sausage waves of wavelength $2\pi/k_z$, as observed in flaring coronal loops.

An initial-value problem is solved with the initial condition

$$V_r(r, t = 0) = A_0 r \exp(-r^2/d^2), \quad (10)$$

where A_0 is the amplitude. This form of the initial perturbation has the sausage symmetry as it is independent of the azimuthal angle ϕ and the plasma velocity at the axis of the cylinder is zero. The width of the perturbation in the radial direction is taken to be sufficiently large to avoid the excitation of higher radial harmonics: the shape of the perturbation is close to the transverse structure of the lowest mode (see, e.g., Pascoe et al. 2007b; Inglis et al. 2009), with one maximum of the radial velocity perturbation in the radial direction. Higher radial sausage harmonics have more than one extremum in the radial direction, and hence are excited by driver (10) less effectively. In the longitudinal direction, the initial perturbation is described by a harmonic function with wavenumber k_z. Equation (10) is supplemented by the boundary conditions $V_r(r = 0, t) = V_r(r = 50d, t) = 0$.

The evolution of the initial perturbation was calculated numerically using the function *pdsolve* of *Maple* 16, which implements a second-order (in space and time) centered finite-difference scheme (see Maple User Manual 2012, for details). The convergence of the method was checked by doubling the number of grid points. The performance of this solver, in particular the radial structure of the sausage mode and its period for a given wavelength, was tested by comparing with the exact analytical results for a similar problem for a zero-β plasma slab with symmetric Epstein profile of the density embedded in a straight magnetic field (Cooper et al. 2003). In the cylindrical case considered in this paper calculations were carried out in the domain ($0 < r < 50d$, $0 < t < NdC_{A\infty}$), where N is sufficiently large (e.g., $N = 50$) for confident resolution of several periods of oscillations.

Two typical scenarios of the evolution of the initial perturbation, leaky and trapped oscillations, are shown in Figure 2. The figure shows the time evolution of the radial structure of the initial impulsive perturbation of the harmonic dependence on the longitudinal coordinate, $\cos(k_z z)$, for an arbitrary value of z. It is evident that in the trapped regime the initial excitation remains localized near the axis of the cylinder ($r = 0$) and is evanescent for higher values of r. In contrast, the leaky waves are radiated from the cylinder to the external medium as propagating fast magnetoacoustic waves. However, they can be seen in the cylinder for some time after the excitation as decaying harmonic oscillations.

By analyzing the signal at a chosen spatial position, e.g., $r = d$, we obtain information about its time evolution and hence the period of oscillations and the decay time. As the signal decays quickly in the leaky regime, the preferred analytical tool is to fit the time signal with an exponentially decaying harmonic function using the least-squares method. In this study we restrict our attention to the analysis of the dependence of the period on the parameters of the cylinder and the initial excitation only.

3. PARAMETRIC STUDY

3.1. Dependence of the Sausage Mode Period on the Longitudinal Wavelength

Figure 3 shows the dependence of the period of sausage oscillations on the wavelength $2\pi/k_z$. In the short-wavelength limit the period is determined by the ratio of the longitudinal wavelength to the Alfvén speed at its center (e.g., Edwin & Roberts 1983). In the figure, this corresponds to the straight line $P = 2\pi/[k_z C_A(r = 0)] = 2\pi/[k_z C_{A\infty}(1 - \delta)]$. With increasing wavelength, the period increases and the effective phase speed is in the range between the Alfvén speed in the center of the cylinder and at infinity, which is consistent with the reasoning in Nakariakov et al. (2003). As the wavelength increases, the growth of the period becomes less steep, gradually approaching another asymptote, $P = 2\pi/(k_z C_{A\infty})$, determined by the Alfvén speed outside the cylinder. An important feature of this dependence is the presence of the cutoff value. At the cutoff, the period is equal to the ratio of the wavelength to the value of the Alfvén speed at infinity.

For wavelengths shorter than the cutoff value, the oscillations are trapped and the period grows with increasing wavelength. This is consistent with the results obtained in the slab geometry (Pascoe et al. 2007b; Inglis et al. 2009). In the weakly leaky regime, for wavelengths slightly exceeding the cutoff value, the period still grows with wavelength (see the right panel of Figure 3), again in agreement with the slab case. For long wavelengths, the dependence of the period on the wavelength shows saturation, and the period becomes independent of

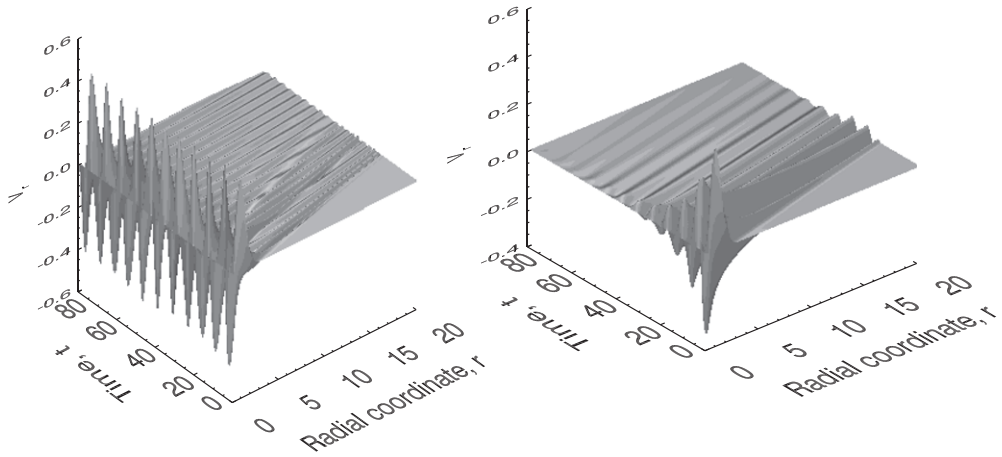

Figure 2. Left panel: example of a trapped oscillation, obtained for the parameters $k_z = 1.5$, $\delta = 0.8$, and $\alpha = 6$. Right panel: example of a leaky oscillation for $k_z = 0.4$, $\delta = 0.7$, and $\alpha = 6$. The time is measured in $d/C_{A\infty}$ and the radial distance in d. The vertical axis shows the radial component of the plasma velocity measured in units of the initial amplitude A_0.

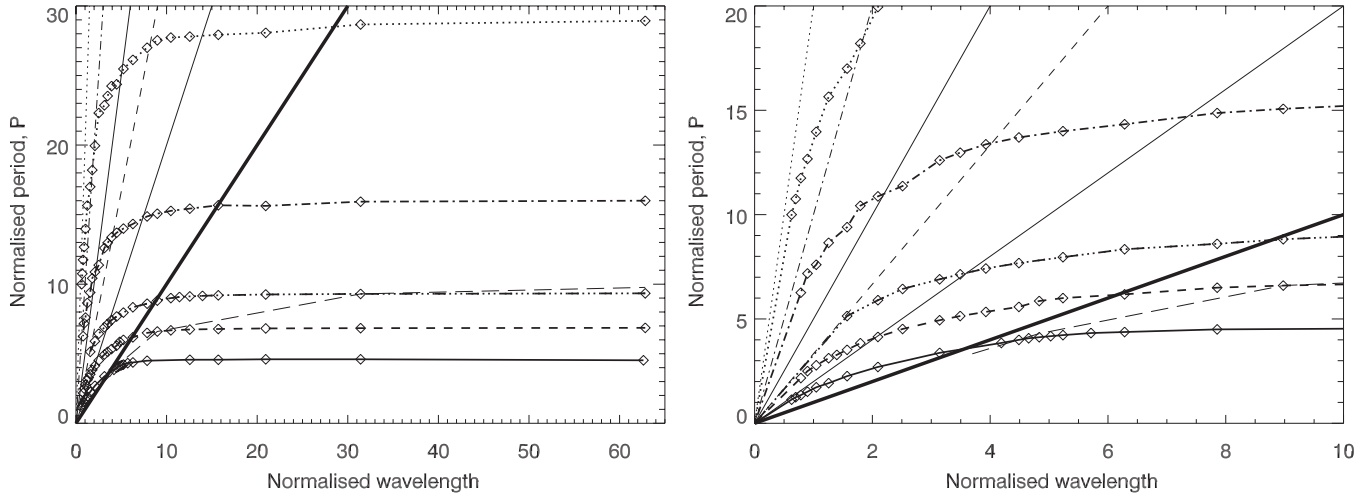

Figure 3. Left panel: dependence of the period of oscillations on the wavelength $2\pi/k_z$ for different values of the parameter δ that is connected with the density contrast inside and outside the cylinder. The dotted curve shows the case of $\delta = 0.95$, the dot-dashed curve $\delta = 0.9$, triple dot-dashed $\delta = 0.8$, dashed $\delta = 0.7$, and the solid line is for $\delta = 0.5$. The diamonds represent the specific measurements. The value of α is 6 for all curves. The thick straight line shows the cutoff, $P = 2\pi/(k_z C_{A\infty})$. Other straight lines show the values of $P = 2\pi/[k_z C_{A\infty}(1-\delta)]$ for the various values of δ. The long dashed line shows where the damping time is equal to three periods of oscillations. The period is measured in units of $d/C_{A\infty}$ and the wavelength in units of d. Right panel: same as in the left panel, but zoomed to show the trapped regime.

wavelength. This effect is more pronounced for cylinders with higher ratios of the external to internal Alfvén speeds, in other words with a deeper potential well in the radial profile of the Alfvén speed. This effect was not found in the slab case (Pascoe et al. 2007b; Inglis et al. 2009) because the wavelengths in the simulations were insufficiently long to see the saturation of the sausage mode period. In all cases considered, for the same values of wavelength and the Alfvén speed at infinity, the sausage mode periods are always longer for cylinders with lower internal Alfvén speed. In the low-β model considered, cylinders with lower internal Alfvén speed are cylinders with denser plasma.

The figure also contains a curve indicating where the damping time is equal to three periods of oscillations. Above this curve, the oscillations are of sufficiently high quality to be easily detectable in the data. Thus, leaky sausage oscillations in long dense loops, with a high ratio of the Alfvén speeds, can also be of sufficiently high quality, with the damping time much longer than the period of oscillations, to be easily detectable in the data. We must point out that the damping considered here is connected with the wave leakage only. In addition, the sausage mode can be subject to damping connected with various dissipative processes, which also reduce the quality of the oscillations. For example, in hot and dense flaring loops field-aligned thermal conduction (Zaitsev & Stepanov 1982) may be such a process. This effect is not considered in our study as our governing equations are ideal.

3.2. Dependence of the Sausage Mode Period on the Steepness of the Transverse Profile

The left panel of Figure 4 shows the effect of the transverse profile steepness on the sausage mode period. As discussed in Section 3.1, for the step-function profile, in the short-wavelength limit the period is determined by the ratio of the longitudinal wavelength to the Alfvén speed at its center. Our calculations confirm this result, which is correct for smooth profiles also. With increasing wavelength, the period growth is lower than the short-wavelength asymptote, $P = 2\pi/[k_z C_{A\infty}(1-\delta)]$. For the same wavelength, the periods of sausage oscillations in

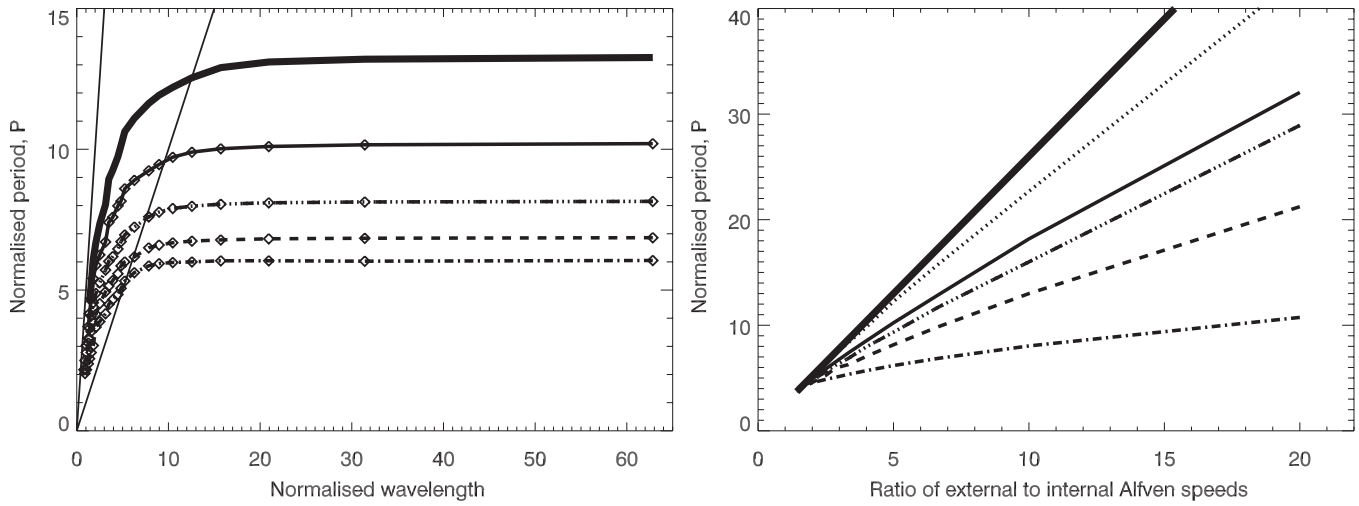

Figure 4. Left panel: dependence of the period of oscillations on the wavelength for different steepnesses of the radial profile α. The thick solid line corresponds to $\alpha = \infty$, the thin solid line to $\alpha = 8$, the triple dot-dashed line to $\alpha = 6$, the dashed line to $\alpha = 4$, and the dot-dashed line to $\alpha = 2$. The value of δ is 0.8 for all curves. The straight lines are the cutoffs $P = 2\pi/(k_z C_{A\infty})$ and $P = 2\pi/[k_z C_{A\infty}(1-\delta)]$. Right panel: dependence of the period, in the long-wavelength limit, on the ratio of external to internal Alfvén speeds for different steepnesses. The dotted curve corresponds to $\alpha = 20$. The other curve styles are the same as in the left panel. The thick solid line shows the analytical solution in the long-wavelength limit for the step-function profile. In both panels, the period is measured in units of $d/C_{A\infty}$ and the wavelength in units of d.

cylinders with smoother Alfvén speed profiles, of lower indices α, are evidently shorter. This effect can be explained as follows. In the case of the step-function profile, the maximum of the perturbation inside the cylinder is situated at the radial distance where the Alfvén speed is equal to its value at the axis of the cylinder. In cylinders with smoothly growing radial Alfvén speed profiles, the speed at that radial distance is higher than at the axis of the cylinder. Hence, the effective phase speed of sausage oscillations in cylinders with smoothly growing Alfvén speed profiles is higher. For the same longitudinal and radial wavelengths, higher values of the effective phase speed give shorter periods.

Also, for steeper profiles, the cutoff value of the wavelength is found to be bigger. For comparison, we show the analytical result obtained for a cylinder with a step-function profile that corresponds to the limit $\alpha \to \infty$ in our consideration. Hence, as one would intuitively expect, cylinders with steeper profiles are better waveguides for fast magnetoacoustic waves of sausage symmetry.

From the left panel of Figure 4 we find that the effect of the radial steepness of the plasma cylinder on sausage oscillations is rather strong. The difference in the values of the sausage mode period between cylinders with a Gaussian ($\alpha = 2$) and a step-function ($\alpha \to \infty$) radial profiles is more than twice as large for a given parameter δ.

3.3. The Long-wavelength Limit

In the right panel of Figure 4 we demonstrate the dependence of the period in the long-wavelength limit, when it becomes independent of the wavelength, on the Alfvén speed (or density) contrast in the cylinder and on the steepness of its radial profile. The period is systematically longer for higher differences between the Alfvén speeds inside and outside the cylinder, and for steeper profiles.

For comparison, we show the analytical result obtained for a cylinder with a step-function profile that corresponds to the limit $\alpha \to \infty$ in our consideration. This shows that in the zero-β limit the period of a long-wavelength sausage mode of a step-function cylinder depends linearly on the value of $1/C_{A0}$,

$$P \approx 2\pi d/2.4C_{A0}, \tag{11}$$

(e.g., Kopylova et al. 2007), which is consistent with our calculations.

It is also evident that for smoother profiles the sausage mode period becomes shorter (see also the discussion in Section 3.2). The period grows with increasing ratio $C_{A\infty}/C_{A0}$, while for smaller values of the steepness parameter α this dependence departs from the linear relationship that appears in the $\alpha \to \infty$ cases. For a fixed value of the ratio of the Alfvén speeds, the dependence of the period on the steepness parameter α is seen to be extremely nonlinear. In particular, for $C_{A\infty}/C_{A0} = 10$, which is a typical value for flaring loops (e.g., Nakariakov et al. 2003), we get an estimated formula

$$P \approx 26.1d \tanh(\lg \alpha). \tag{12}$$

This is applicable to low-β profiles steeper than Gaussian, $\alpha > 2$, and is consistent with the analytical result in the $\alpha \to \infty$ limit.

4. CONCLUSIONS

We performed numerical simulations of the azimuthally symmetric initial-value problem for a field-aligned low-β plasma cylinder with a smooth radial profile of the density (and hence of the Alfvén speed). The plasma cylinder was excited by a symmetric perturbation of the radial velocity of the plasma and of a harmonic shape in the longitudinal direction. Fast magnetoacoustic sausage modes were found to be easily excited in both trapped and leaky regimes. The results obtained can be summarized as follows.

1. With increasing longitudinal wavelength, the period of the sausage oscillations always grows but this dependence is saturated in the long-wavelength limit.
2. In the trapped regime, the period lies between two values, corresponding to the ratio of the effective radius of the cylinder and the Alfvén speed at its axis and at infinity, and grows increasing wavelength.

3. For wavelengths greater than the cutoff value, sausage modes become leaky. In response to an impulsive excitation in the cylinder, the leaky waves show decaying oscillatory behavior with a period determined by the parameters of the cylinder (the Alfvén speed contrast ratio and steepness). Outside the cylinder, the leaky waves form a wavetrain pattern that propagates outward at the external Alfvén speed. As expected, deeper and steeper profiles of the Alfvén speed correspond to more efficient trapping of sausage modes: the cutoff value of the wavelength increases with steepness and the density (or Alfvén speed) contrast ratio.
4. In the leaky regime, the period is always longer than the period of a trapped mode of shorter wavelength, and also is longer than the cutoff value (the ratio of the wavelength and the Alfvén speed far from the cylinder). For shallow profiles of the density (and hence the Alfvén speed) and shorter wavelengths, the period grows with wavelength in the leaky regime also. In the long-wavelength limit, the period becomes independent of wavelength and is determined by the depth and steepness of the radial profile of the Alfvén speed: the period is approximately inversely proportional to the internal value of the Alfvén speed and depends on the steepness index α as $\tanh(\lg \alpha)$.

Our findings resolve the longstanding problem of the dependence or independence of the period of sausage oscillations on wavelength. Indeed, for shorter wavelengths, even in the leaky regime, the period grows with wavelength. In particular, for thick flaring coronal loops with a density contrast of about 10 (and hence with an Alfvén speed contrast ratio of about 3.16) and a length of about 5–6 times their diameters, as considered by Nakariakov et al. (2003) and Aschwanden et al. (2004), the period of the fundamental sausage mode indeed increases with wavelength. But for longer wavelengths (and higher density contrast ratios), the dependence of the period on wavelength experiences saturation and becomes consistent with the analytical results obtained by Zaitsev & Stepanov (1982) and Kopylova et al. (2002, 2007). Thus, we infer that opposing conclusions drawn previously concerning the dependence of the sausage mode period on wavelength were based on different ranges of the parameters of the problem, and hence are not contradictory. More specifically, the regime described in Pascoe et al. (2007b) and Inglis et al. (2009) corresponds to segments of the solid and dashed curves near the thick solid line in Figure 3 (right panel). On the other hand, the regime described in Zaitsev & Stepanov (1982) and Kopylova et al. (2002, 2007) corresponds to the saturation of the curves in the long-wavelength part of that figure.

This result has important implications for the seismological diagnostics of plasmas in flaring loops with the use of sausage oscillations. In particular, the pronounced dependence of the sausage oscillation period on the steepness of the radial profile of the Alfvén speed provides us with a tool for probing that parameter. The transverse steepness is vital for the assessment of the efficiency of kink wave damping in the solar corona (see, e.g., Goossens et al. 2012 and references therein) and of associated coronal heating. An additional advantage of seismological techniques utilizing the sausage mode is provided by its independence of the length of the loop in the long-wavelength regime. This allows one to exclude this parameter from consideration in the diagnostics of long dense loops. Moreover, Equation (12) gives us a tool for probing the transverse profile of the Alfvén speed and density of sausage oscillations in a coronal loop provided we are able to get independent measurements of the loop diameter d and the Alfvén speed C_{A0}. In particular, the latter parameter can come from the observation of a kink oscillation of the same loop.

This work was supported by the Royal Society UK–Russian International Joint Project, the Marie Curie PIRSES-GA-2011-295272 RadioSun project, and the Russian FCPK-1.5 No. 8524 project. V.F.M. acknowledges grants 02-11-91175 and 02-12-00616 of the Russian Foundation for Basic Research.

REFERENCES

Aschwanden, M. J., Nakariakov, V. M., & Melnikov, V. F. 2004, ApJ, 600, 458
Banerjee, D., Erdélyi, R., Oliver, R., & O'Shea, E. 2007, Sol. Phys., 246, 3
Cally, P. S. 1986, Sol. Phys., 103, 277
Cooper, F. C., Nakariakov, V. M., & Williams, D. R. 2003, A&A, 409, 325
De Moortel, I., & Nakariakov, V. M. 2012, Phil. Trans. R. Soc. A, 370, 3193
Edwin, P. M., & Roberts, B. 1983, Sol. Phys., 88, 179
Goossens, M., Andries, J., Soler, R., et al. 2012, ApJ, 753, 111
Gruszecki, M., Nakariakov, V. M., & Van Doorsselaere, T. 2012, A&A, 543, A12
Inglis, A. R., Nakariakov, V. M., & Melnikov, V. F. 2008, A&A, 487, 1147
Inglis, A. R., van Doorsselaere, T., Brady, C. S., & Nakariakov, V. M. 2009, A&A, 503, 569
Kopylova, Y. G., Melnikov, A. V., Stepanov, A. V., Tsap, Y. T., & Goldvarg, T. B. 2007, Astron. Lett., 33, 706
Kopylova, Y. G., Stepanov, A. V., & Tsap, Y. T. 2002, Astron. Lett., 28, 783
Maple User Manual, Waterloo Maple Inc. 2012, http://www.maplesoft.com/documentation_center
Mathioudakis, M., Seiradakis, J. H., Williams, D. R., et al. 2003, A&A, 403, 1101
Melnikov, V. F., Reznikova, V. E., Shibasaki, K., & Nakariakov, V. M. 2005, A&A, 439, 727
Mossessian, G., & Fleishman, G. D. 2012, ApJ, 748, 140
Nakariakov, V. M., & Melnikov, V. F. 2009, Space Sci. Rev., 149, 119
Nakariakov, V. M., Melnikov, V. F., & Reznikova, V. E. 2003, A&A, 412, L7
Nakariakov, V. M., Roberts, B., & Murawski, K. 1997, Sol. Phys., 175, 93
Pascoe, D. J., Nakariakov, V. M., & Arber, T. D. 2007a, Sol. Phys., 246, 165
Pascoe, D. J., Nakariakov, V. M., & Arber, T. D. 2007b, A&A, 461, 1149
Pascoe, D. J., Nakariakov, V. M., Arber, T. D., & Murawski, K. 2009, A&A, 494, 1119
Roberts, B., Edwin, P. M., & Benz, A. O. 1984, ApJ, 279, 857
Rosenberg, H. 1970, A&A, 9, 159
Ruderman, M. S., & Roberts, B. 2006, Sol. Phys., 237, 119
Selwa, M., Murawski, K., & Kowal, G. 2004, A&A, 422, 1067
Srivastava, A. K., Zaqarashvili, T. V., Uddin, W., Dwivedi, B. N., & Kumar, P. 2008, MNRAS, 388, 1899
Stepanov, A. V., Zaitsev, V. V., & Nakariakov, V. M. 2012, Coronal Seismology (1st ed.; Weinheim: Wiley-VCH)
Su, J. T., Shen, Y. D., Liu, Y., Liu, Y., & Mao, X. J. 2012, ApJ, 755, 113
Van Doorsselaere, T., De Groof, A., Zender, J., Berghmans, D., & Goossens, M. 2011, ApJ, 740, 90
Verwichte, E., Foullon, C., & Nakariakov, V. M. 2006, A&A, 449, 769
Zaitsev, V. V., & Stepanov, A. V. 1975, Issled. Geomagn. Aeron. Fiz. Solntsa, 37, 3
Zaitsev, V. V., & Stepanov, A. V. 1982, Sov. Astron. Lett., 8, 132